Al-Kitab Journal for Pure Sciences (2026); 10(2):221-241.
https://doi.org/10.32441/kjps.10.2.p16

Al-Kitab Journal for Pure Sciences
ISSN: 2617-1260 (print), 2617-8141(online)

https://isnra.net/index.php/kjps

Synthesis And Characterization and Anti-Cancer Activity of Nickel (II) Complexes Containing a Mixture of Benzotriazole Derivative, Phenanthroline , and Bipyridine, and Evaluation of Their Bioavailability

Alaa H. Ali

Iraq's Ministry of Education's General Directorate of Education in Salah al-Din

Corresponding Author: Alaa.hamad.ali@st.tu.edu.iq

Citation: *Alaa H. Ali*[1]. **Synthesis And Characterization and Anti-Cancer Activity of Nickel (II) Complexes Containing a Mixture of Benzotriazole Derivative, Phenanthroline, And Bipridine, And Evaluation of Their Bioavailability.**
Al-Kitab J. Pure Sci. [Internet]. 2026 May. 24 ;10(2):221-241
DOI.
https://isnra.net/index.php/kjps/article/view/2026.
https://doi.org/10.32441/kjps.10.2.p16

Keywords: Benzatriazole, Phenonthroline, and Bipyridine biological effectiveness, anti-cancer, Ni (II) complexes.

Article History
Received 21 Apr. 2026
Accepted 24 May. 2026
Available online 01 Nov. 2026

©20--. THIS IS AN OPEN-ACCESS ARTICLE UNDER THE CC BY LICENSE
http://creativecommons.org/licenses/by/4.0/

Abstract:

The study of inorganic chemistry, particularly coordination chemistry, has become increasingly important in recent years due to its significant advancements in the scientific field of preparing and characterizing coordination complexes. Coordination compounds have attracted considerable attention from researchers because of their crucial role in various aspects of life. These complexes have been used extensively in medicine, industry, agriculture, and even in the field of Pollution. The formation of these complexes involves transition elements and representative elements, but they are particularly observed with transition element ions. This is because they provide empty orbitals, and their orbital energies are lower than those of the nonmetal atoms involved in the ligand structure, which possesses non-shared electron pairs capable of bonding with the metal ion.

Nickel is the eighth element of the first transition series (3d elements), and it has an outer electron configuration ($4s^2$ $3d^8$). The stability of its compounds decreases as its oxidation state increases, and the oxidation state (II) is one of the most stable states of nickel. Therefore,

nickel(II) is the most common in the chemistry of transition elements, but it is not easy to work with because of the changes that occur in the structure of some octahedral, tetrahedral, and square planar complexes, as well as the formation of polymers.

Keywords: Benzatriazole, Phenonthroline, and Biperidine biological effectiveness, anti-cancer, Ni (II) complexes.

تحضير وتشخيص ودراسة النشاط المضاد للسرطان لمعقدات النيكل (II) الحاوية على مزيج من مشتق البنزاترايازول والفينونثرولين والبايبريدين وتقييم فعاليتها الحيوية

علاء حمد علي

وزارة التربية، المديرية العامة لتربية صلاح الدين

الإيميل الرسمي: Alaa.hamad.ali@st.tu.edu.iq

الخلاصة:

ازدادت أهمية دراسة الكيمياء غير العضوية، ولا سيما كيمياء التناسقية ، في السنوات الأخيرة نظرًا للتقدم الكبير الذي أحرزته في مجال تحضير وتوصيف معقدات التناسق. وقد حظيت هذه المعقدات باهتمام بالغ من الباحثين لدورها المحوري في مختلف جوانب الحياة. وتُستخدم هذه المعقدات على نطاق واسع في الطب والصناعة والزراعة، وحتى في مجال مكافحة التلوث . يتضمن تكوين هذه المعقدات عناصر انتقالية وعناصر تمثيلية، ولكنها تُلاحظ بشكل خاص مع أيونات العناصر الانتقالية. ويعود ذلك إلى توفيرها مدارات فارغة، وانخفاض طاقات مداراتها مقارنةً بذرات اللافلزات المشاركة في بنية الرابطة، والتي تمتلك أزواجًا إلكترونية غير مشتركة قادرة على الارتباط بأيون الفلز.

النيكل هو العنصر (الثامن في السلسلة الانتقالية الأولى) عناصر (3d)، وله توزيع إلكتروني .($4s^2\ 3d^8$) يقل استقرار مركباته مع ازدياد حالة أكسدته، وتُعد حالة الأكسدة (II) من أكثر حالات الأكسدة استقرارًا للنيكل. لذلك، فإن النيكل (II) هو الأكثر شيوعًا في كيمياء العناصر الانتقالية، ولكنه ليس من السهل العمل معه بسبب التغيرات التي تحدث في بنية بعض المركبات ثمانية السطوح، ورباعية السطوح، والمربعة المستوية، بالإضافة إلى تكوين البوليمرات .

الكلمات المفتاحية: بنزوترايوزول , فينونثرولين و بايبريدين, فعالية بايلوجية ودراسة مضادة للسرطان لمعقدات النيكل(II).

1. Introduction:

Benzotriazole ($C_6H_5N_3$) represents a versatile N-heterocyclic ligand widely recognized in coordination chemistry for its strong electron-donating capabilities and diverse coordination modes [(1)]. Possessing adjacent nitrogen atoms, it effectively coordinates with transition metal ions—particularly intermediate Lewis acids like nickel, Ni(II) to assemble structurally unique complexes and polymeric architectures [(2)]. Beyond structural intrigue, the integration of Ni(II) centers with benzotriazole derivatives enhances biomolecular interactions, often leading to potent cytotoxicity against specific cancer cell lines [(3)]. In particular, evaluating the in vitro

antiproliferative activity of these metal complexes against human breast adenocarcinoma (MCF-7) offers critical insights into their targeted anticancer potential [٤]. Consequently, the synthesis and biological screening of novel Ni(II) benzotriazole complexes continue to serve as a promising direction in bioinorganic and medicinal chemistry [5].

Nickel (Ni) complexes with Schiff base ligands represent a pivotal class in modern coordination chemistry due to their facile synthesis, structural flexibility, and high thermodynamic stability. These complexes efficiently coordinate through multi-donor atoms such as nitrogen and oxygen (N,O-donor systems), exhibiting versatile coordination geometries alongside tailored electronic and catalytic properties [6]. Recently, they have shown promising potential in clean energy technologies, including electrochemical systems and hydrogen storage applications, owing to their robust structural stability and redox behaviors [7]. Furthermore, Schiff base nickel complexes display significant biological efficacy as potent antibacterial, antifungal, and anticancer agents, positioning them as valuable candidates for advanced pharmaceutical and technological research [8].

2-Experimental

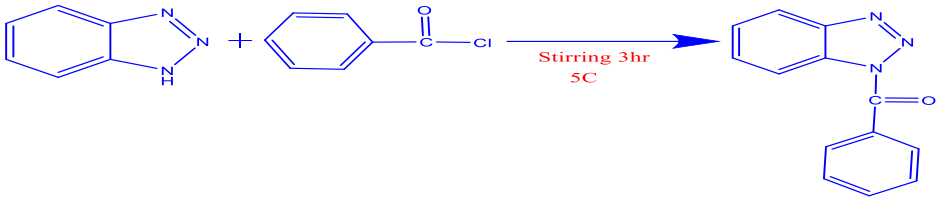
An automatic melting point device (SAM30) was used to determine the melting point of the produced compounds. A SHIMADZU 8400S spectrometer was used to record the complexes' infrared spectra (FT-IR) as discs (KBr) (within the range 400-4000 cm^{-1}). The nuclear magnetic resonance spectrum was recorded using a Varian Unity Spectrometer (400 MHz) in DMSO-d6 solvent. The properties of the thick or thin samples of the material, their shape, and the determination of their nanoscale or crystalline dimensions of the particles were determined using a TESCAN MIRA3 instrument.

3. Material and methods:

3.1 Preparation methods:

3-1-1 The ligand is prepared using (L)((H-benzo[d][1,2,3]triazol-1-y)(phenyl) methanone

a suspension of 3 g (0.02581 mol) benzotriazole solution dissolved in 15 ml of absolute ethanol, stirring until dissolved, in an ice bath. Then add 3 ml (0.02581 mol) of benzyl chloride drop by drop. The temperature should not exceed 0–5°C. The solution changed from clear to a thick white suspension and was left to stir for four hours. The material was filtered and allowed to dry at room temperature. The weight was 3.7008 g, the melting point was 106–109 C^0, and the concentration was Yield 85% [9].



3-1-2 Preparation of the complex $[Ni(L)_2Cl_2]$

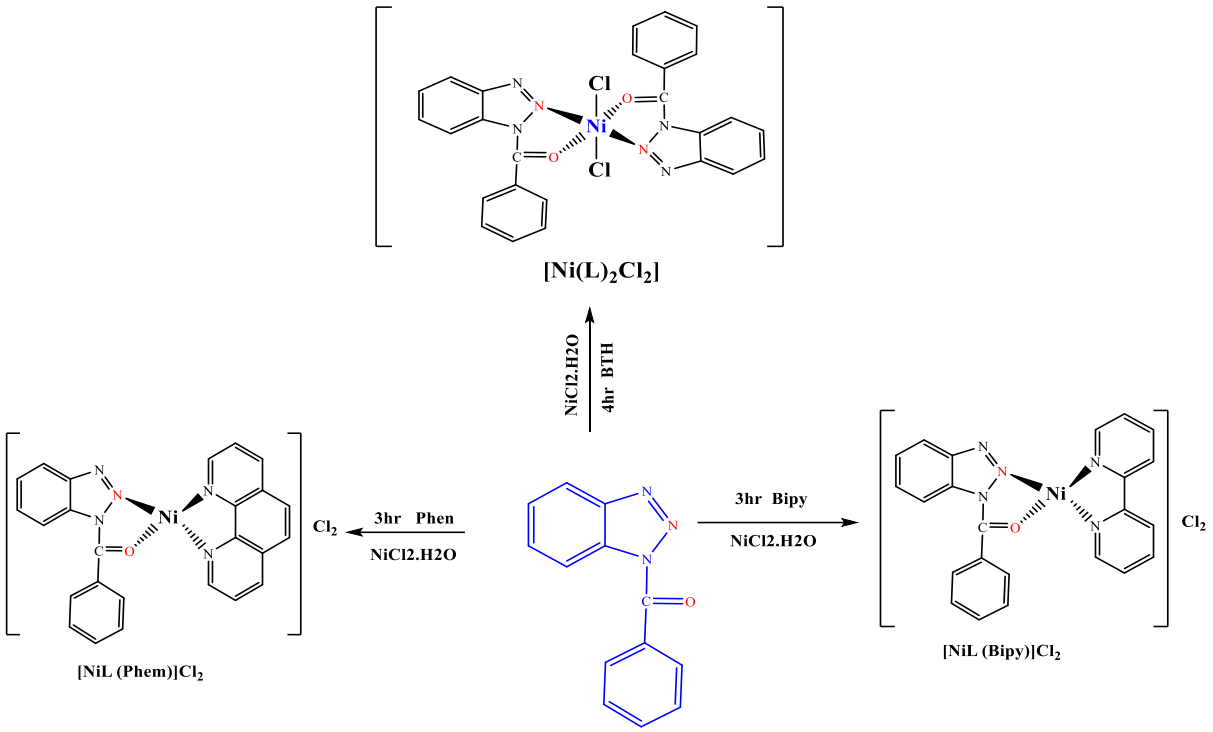
A hot, green solution of (0.026g, 0.00011mmol) in (5ml) of ethanol was added to a ligand solution (L) of (0.05g, 0.00022mmol) in (5ml). A suspension was formed. The mixture was heated under a temperature of 80°C for two hours, then the precipitate was filtered and washed with cold ethanol and left to dry at room temperature (wt=0.055g, Yield =72%, m.p=240-243°C).

3-1-3 Preparation of the $[Ni(L)(Phen)]Cl_2$ complex

A suspension of (L) (0.531 gm, 0.00237 mol) in absolute ethanol (10 ml) was added to a solution of nickel chloride ($NiCl_2$) (0.839 gm, 0.00237 mol) in ethanol (15 ml). The mixture was stirred for one hour, then a solution of (10,1 phenanthroline) (0.427 gm, 0.00237 mol) in ethanol (20 ml) was added. The final mixture was raised for three hours, resulting in a light green suspension. The precipitate was filtered, washed with cold ethanol, and oven dried under reduced pressure (1.578gm , Yield =87.81% , M.P 275-278).

3-1-4 Preparation of the $[Ni(L)(Bipy)]Cl_2$ complex

A suspension of (L) (0.121 gm, 0.00054 mol) in absolute ethanol (10 ml) was added to a solution of nickel chloride ($NiCl_2$) (0.190 gm, 0.00054 mol) in ethanol (15 ml). The mixture was stirred for one hour, then a solution of (2,2'-biperidine) (0.082 gm, 0.00054 mol) in ethanol (20 ml) was added. The final mixture was raised for three hours, resulting in a light green suspension. The precipitate was filtered, washed with cold ethanol, and oven dried under reduced pressure (0.350 g, Yield =89.05%,, M.P 280-282).



Complex diagram :(1:1) $[Ni(L)Cl_2]$, $[Ni(L)(Bipy)]Cl_2$, $[Ni(L)(Phen)]Cl_2$

4. Evaluate bacterial activity:

4-1 Evaluate the bacterial activity of the prepared complexes:

The biological activity of the prepared complexes was tested on two types of bacteria: Gram-negative and Gram-positive, using the etching method. The bacterial isolates used were identified by the Department of Life Sciences, College of Science, University of Mosul.

1) *Citrobacter freundii* (Gram-Negaive)
2) *staphlycocas aureus* (Gram-positive)
3) *(Staphylococcus epidermidis)* (Gram-positive)

4-1-1 Method of operation:

The complex solutions were prepared using DMSO solvent at concentrations of (10^{-1}, 10^{-3}, 10^{-5}). The culture medium was then prepared. The bacteria were activated by dissolving (15gm) of nutrient agar in (0.5L) of distilled water and placing it in a conical flask. The mixture was mixed well and heated until the agar (a gelatinous substance used as a nutrient medium for bacterial growth) was completely dissolved. After that, the culture medium was placed in a sterilizer at a temperature of (121^0C) and a pressure of (15 bar) for 15 minutes [10]. Then, after removing it, it was poured into Petri dishes and left to solidify. After that, (3-5) smears of the prepared bacterial samples were placed and incubated for 24 hours at 37 degrees Celsius in the incubator. Then, the culture medium used to evaluate biological activity was prepared by

dissolving (53.5gm) of Mueller-Hinton agar in (1L) of distilled water. Then, the medium was placed in a sterile device (Autoclave) at a temperature of (121°C) and a pressure of (15 bar) for 15 minutes [11].

The medium is extracted after sterilization in an autoclave and poured into Petri dishes. It is then left to solidify. A quantity of activated bacteria is taken by swab and applied to the Mueller-Hinton agar medium by completely covering the dish and marking it. It is left for half an hour to absorb [12]. Then, holes are prepared using a sterile cork drill with a diameter of 5 mm. Four holes are made, and 1 ml of the prepared compound solutions is added to each hole at different concentrations. All dishes are then incubated for 24 hours. The antibiotic cefepime is used at a concentration of 5-10^{-5} M, and its inhibition of the bacteria is observed [13] .The diameter of the inhibition zone for each complex is then measured using a millimeter ruler and compared with the inhibition range of the antibiotic cefepime [14].

5. Results: and Discussion :

This research involves the preparation and characterization of several nickel(II) complexes, piperidine ligands, and phenenthroline coligands. The prepared complexes were characterized using several physical and spectroscopic methods. The following ligands were used in this research:

1) ((H-benzo[d][1,2,3]triazol-1-y)(phenyl)methanone)) (L)
2) 2,2-Bipyridyl (**Bipy**)
3) 1,10-phenanthroline (**Phen**)

5.1 Molar Conductivity :

The molar conductivity of solutions is widely used in coordination chemistry to determine the ionic formulas of complexes in solution and in the solid state. The greater the number of ions released by the complex in solution, the higher its electrical conductivity. A complex that does not ionize has a low conductivity that can be neglected [15]. The electrical conductivity of the prepared complexes was measured at a concentration of (10^{-3} M) in dimethyl sulfoxide (DMSO) solutions at room temperature (25°C), as shown in the table [16].

The molar conductivity results for the prepared (L) ligand complexes showed values ranging from 67.3 to 78.6 ohm^{-1} cm^{-2} mol^{-1}, indicating the presence of two Cl ions within the coordination sphere. In contrast, the $[Ni(L)Cl_2]$ complexes, where we expect two Cl ions to be

present outside the coordination sphere, showed values ranging from 75.4 to 78.6. This is consistent with the proposed formulas and supported by other analyses and measurements. Table (1-1) shows the results of the molar electrical conductivity measurements for the prepared complexes [17].

Table 1-1. Physical properties, melting points, percentage yields, and molar conductivity values of the synthesized ligand and its Ni(II) complexes.

Seq	Complexes	Color	M.P.C°	Yield %	Conductivity ohm^{-1}.cm^{-2} .mol^{-1}
---	L	صحراوي	106-109	85.9	2.0
1	$[Ni(L)_2Cl_2]$	احضر	240-243	72	67.3
2	$[Ni(L)(Phen)]Cl_2$	اخضر فاتح	275-278	87.8	75.4
3	$[Ni(L)(Bipy)]Cl_2$	اخضر فاتح	280-282	89.05	78.6

5.2 Infrared Spectrum of the (L) Complex

The ligand was identified by infrared spectroscopy. As shown in figure (1-2). The infrared spectrum of the free ligands showed the disappearance of the (N-H) υ[18] band at position (3415cm), and the clear appearance of the C=O) υ band at position (1708cm) cm[19], as well as the appearance of the aromatic C-H) υ band[20] at position (3060 cm^{-1}) and the appearance of a band belonging to (N=N) at position (1448 cm^{-1}) [21].

5-2-1 Nuclear Magnetic Resonance Spectrum ^{1} Hnmr for (L) ligand

The proton nuclear magnetic resonance spectrum of the 1H NMR ligand, as shown in figure (1-3), measured with DMSO-d6 solvent, showed a multiple signal within the chemical shift (8.35-7.60ppm) δH, which is due to the aromatic (C-H) of the nine protons of the ligand, and the appearance of a triple signal at the chemical shift (8.32ppm) δH, which is due to protons 5 and 9, and a double signal at the chemical shift (8.12ppm) δH, which is due to protons 1 and 4, and two triple signals at the shifts (7.85ppm and 7.82ppm) δH, respectively, which are due to protons 2 and 3, and a multiple signal within the chemical shift (7.66ppm) δH, which is due to protons (6, 7, 8).

5-2-2 Nuclear Magnetic Resonance Spectrum ^{13}C-^{1}H N.m.r of the (L) ligand

The ^{13}C-{^{1}H}NMR spectrum of the ligand, as shown in figure (1-4), measured with DMSO-d6 solvent, showed a carbon atom signal of the carbonyl group (C=O) at a displacement of

δC=167.09 ppm. This signal appeared in this region due to the high electronegativity of oxygen. The other signals are due to the remaining 12 carbon atoms of the ligand.

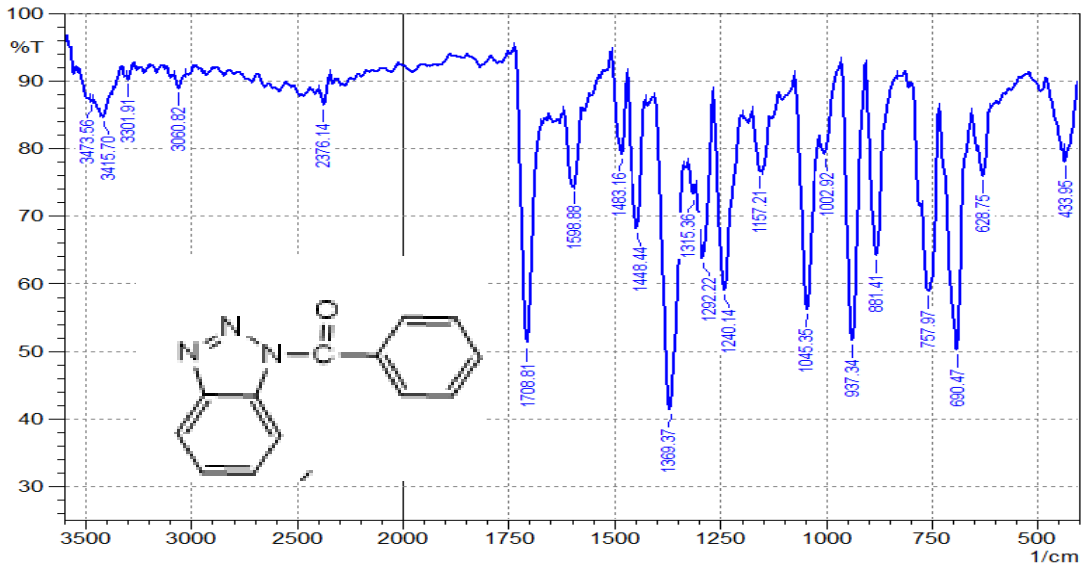


Figure (1-2) – Infrarotspektrum des Liganden (L)

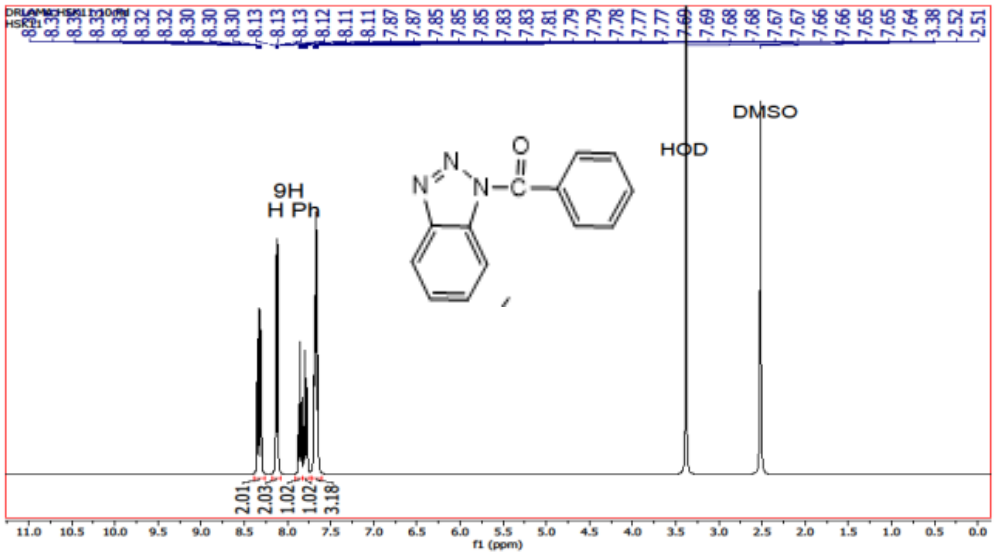


Figure (1-3) ^{1}H NMR spectrum of the L complex

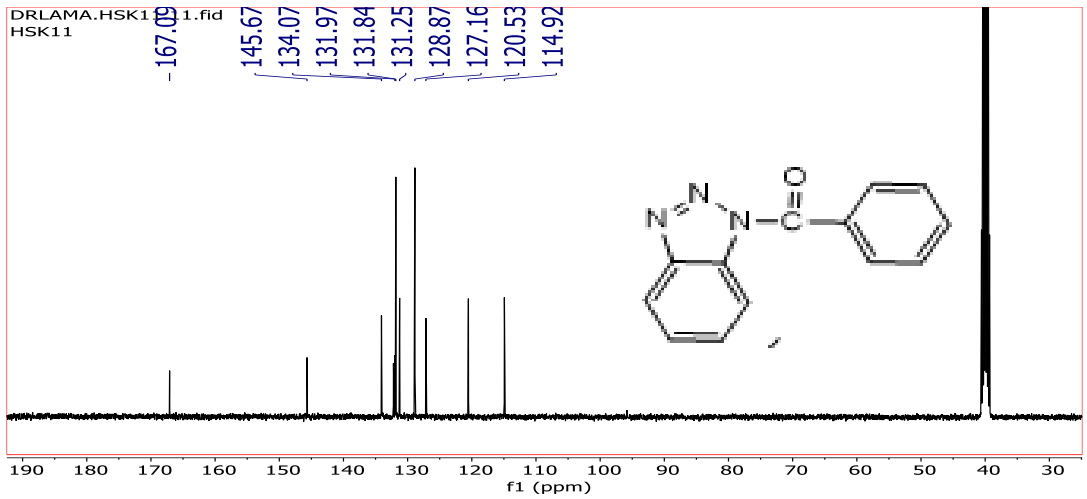


Figure (1-4) ^{13}C-{1H} NMR spectrum of the L complex

5-2-3 Infrared spectrum the [Ni(L)Cl$_2$]

The infrared spectrum of the Ni(L)Cl$_2$ complex, as shown in figure (1-5) , showed a band at position (3066cm^{-1}) corresponding to the aromatic (C-H) frequency [20]. A strong band was also observed at(1606cm-^{1}) corresponding to the stretching frequency of the (C=O) group [19], as well as a band at position (485cm-^{1}) corresponding to the (N=N) frequency [21]. A band was also observed at position (547cm^{-1}) corresponding to the (Ni-O) frequency, a band at position (449 cm-^{1}) corresponding to the (Ni-N) frequency, and a band at position (1267 cm-^{1}) corresponding to the (C-N) frequency [22].

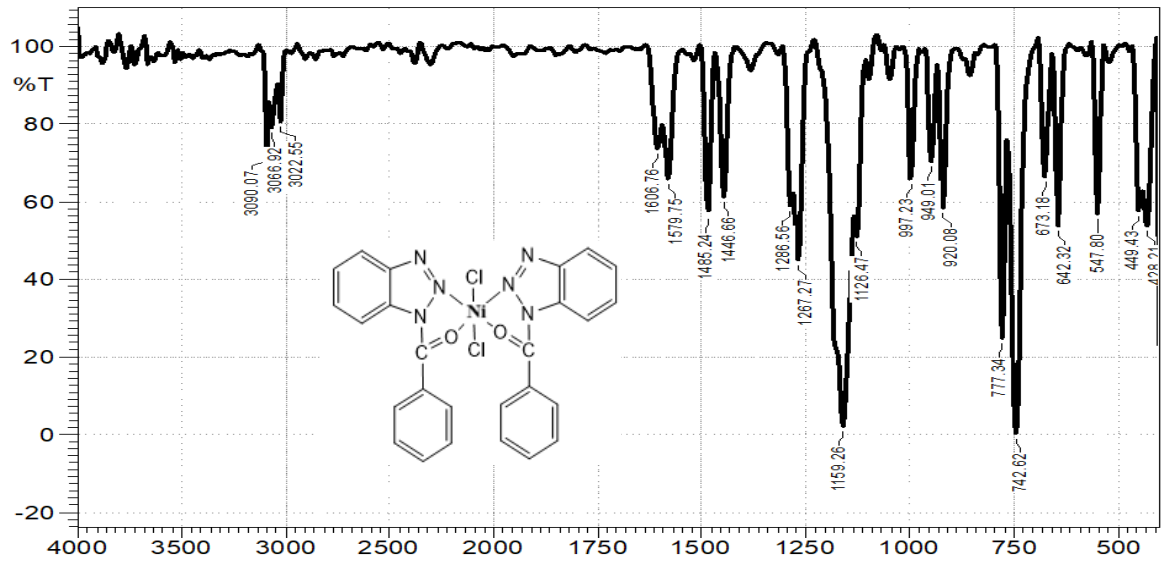


Figure (1-5) IR spectrum of the [Ni(L)Cl$_2$]

5-2-4 Spectrum of Nuclear Magnetic Resonance {^{1}H} n.m.r of the [Ni(L)Cl$_2$] complex

The proton nuclear magnetic resonance spectrum of the 1H NMR ligand, as shown in figure (1-6), measured in DMSO-d^6 solvent, showed a triplet signal within the chemical displacement (8.30-8.41 ppm) δH with approximately two protons, which is due to a proton in a, a doublet signal within the displacement (8.1-8.2 ppm) δH, which is due to a proton in b, a multiplet signal within the chemical displacement (7.80-7.90 ppm) δH, which is due to a proton in d, a singlet signal at (7.60-7.65) δH, which is due to the protons of C, and a triplet signal within the chemical displacement (7.65-7.70 ppm) δH, which is due to a proton in e.

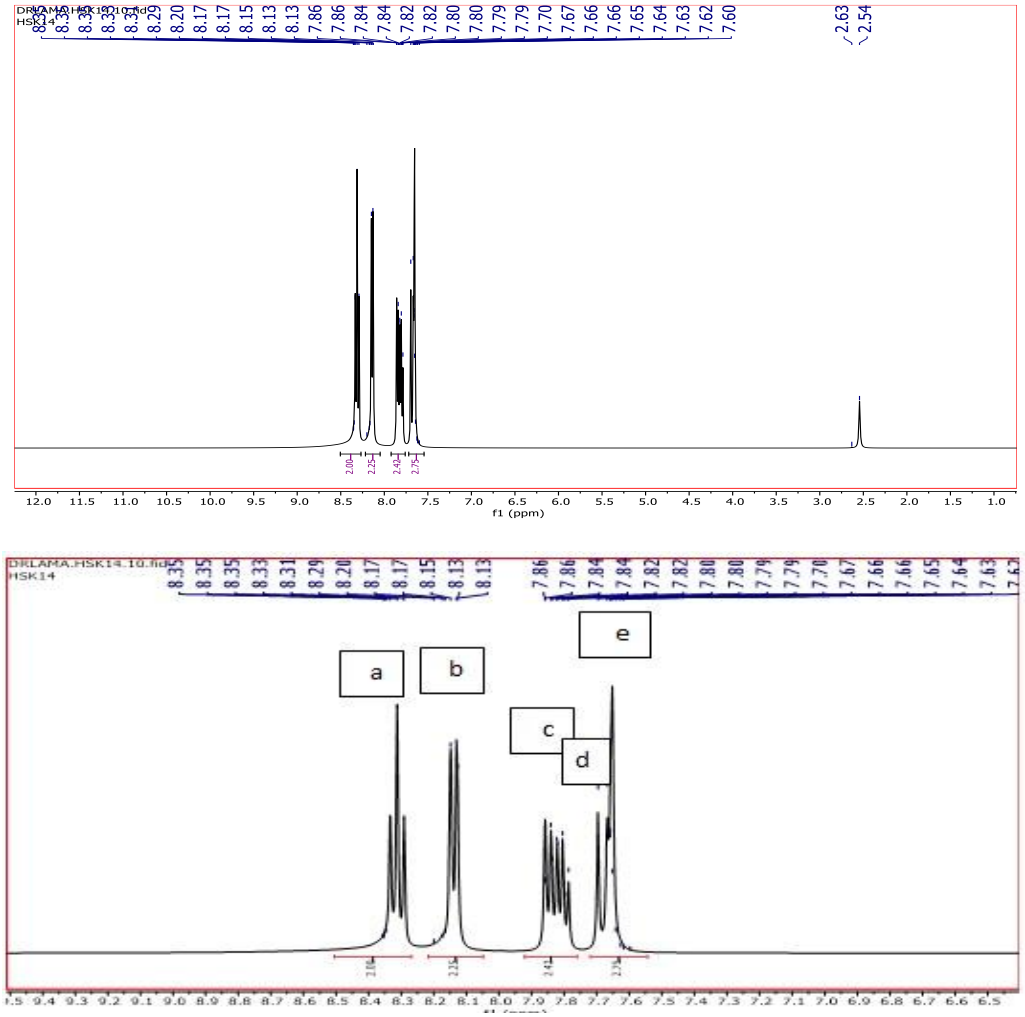


Figure (1-6) Spectrum of nuclear magnetic resonance (^{1}H-NMR) of the Ni(L)Cl$_2$ complex

5-2-5 Infrared spectra of the complex [Ni(L)(phen)]Cl$_2$

The infrared spectrum showed a sharp and strong beam within the range (1672 cm^{-1}) which is attributed to the stretching frequency of the (C=N) group within the ring [23]. and the appearance of a beam within the range (2979 cm^1) which is attributed to the aliphatic (C-H)

group[24], and a beam at the range (3060 cm^{-1}) which is attributed to the aromatic (C-H) group [20], and the appearance of a beam at (1421 cm^{-1}) which is attributed to the stretching frequency of the (N=N) group υ [21], and a sharp beam at (1618 cm^{-1}) which is attributed to the stretching frequency of the (C=C) group υ[26] , as well as a beam within the range (1672 cm^{-1})[25][27] which is attributed to the (C=N) group in the (Phen) ligand. Additionally, the remaining bands appear in their positions, as shown in Figure (1-7).

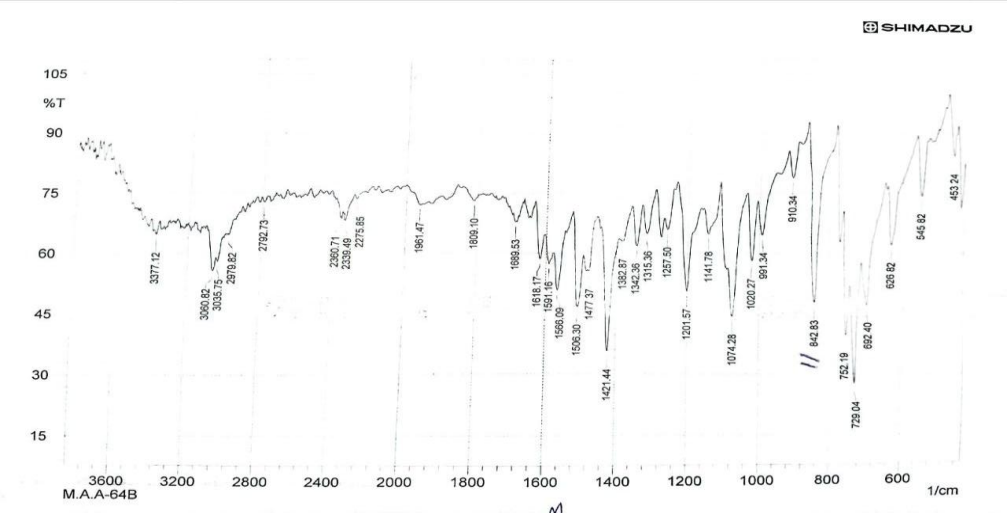


Figure (1-7) IR spectrum of the ligand [Ni(L)(phen)]Cl_2

5-2-5- ^{1}H nmr NMR spectrum of the [Ni(L)(phen)]Cl_2 complex

The proton NMR spectrum of the complex measured with DMSO-d^6 solvent showed that the Phen proton signals exhibited a single signal at (**δ**H=8.1 ppm) with two protons complemented and attributed to a proton at position H4; a double signal at (**δ**H=8.27 ppm) with two protons complemented and coupling constants ($^3J_{H2-H3}$=8.2 Hz) and ($^4J_{H2-H1}$=4.65 Hz) attributed to a proton at position H2; a double signal at (**δ**H=8.8 ppm) with two protons complemented and coupling constants ($^3J_{H3-H2}$=8.16 Hz) and ($^4J_{H3-H1}$=1.56 Hz) attributed to a proton at position H3; and a broad single signal at (**δ**H=9.1 ppm) with two protons complemented and attributed to a proton H1. as shown in Figure (1-8).

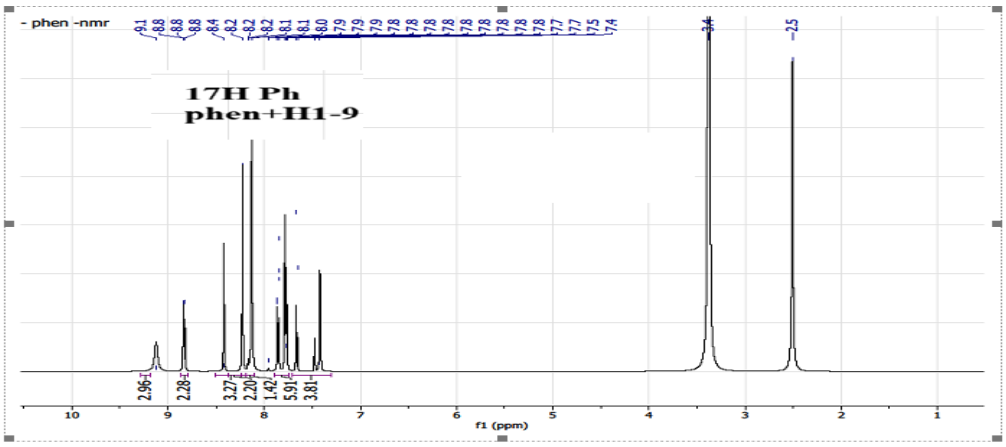


Figure (1-8) ^{1}H nm NMR spectrum of the [Ni(L)(phen)]Cl_2 complex

5-2-6 Infrared spectra of the complex [Ni(L)(Bipy)]Cl_2

The infrared spectrum showed a sharp, strong band in the range of 1672 cm^{-1}, which corresponds to the stretching frequency of the C=N group within ring [23]. A band in the range of 2996 cm^{-1} was attributed to the aliphatic C-H group, and another band in the range of (3066 cm^{-1})[24] was attributed to the aromatic C-H group [20]. A further band in the range of 1446 cm^{-1} was attributed to the C=N group in the Bipy ligand [28], which shifted to a lower frequency than in the free ligand, specifically at (1672 cm^{-1}). This shift indicates a bidental chelate symmetry of Phen with the metal. The remaining bands appeared in their respective positions, as shown in Figure (1-9).

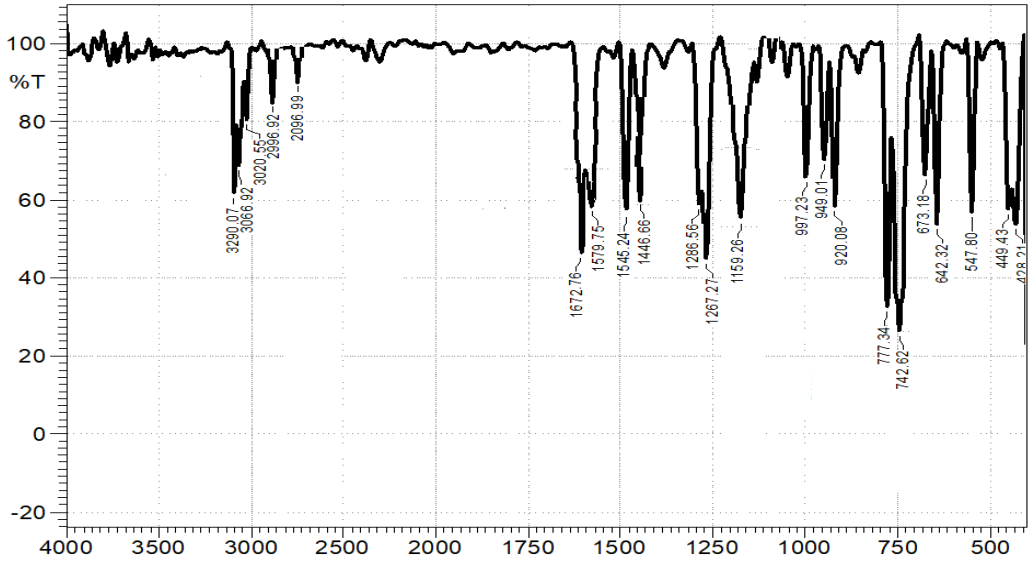


Figure (1-9) Infrared spectrum of the ligand [Ni(L)(Bipy)]Cl_2

5-2-7 ^{1}H nmr Nuclear Magnetic Resonance Spectrum of the [Ni(L)(Bipy)]Cl_2 complex

The proton NMR spectrum of the complex measured with DMSO-d^6 solvent showed that the proton Bipy signal exhibited a single signal at (**δ**H=8.11 ppm) with two protons complemented and attributed to a proton at position H4; a double signal at (**δ**H=8.26 ppm) with two protons complemented and coupling constants ($^{3}J_{H2-H3}$=8.2 Hz) and ($^{4}J_{H2-H1}$=4.65 Hz) attributed to a proton at position H2; a double signal at (xH=8.25 ppm) with two protons complemented and coupling constants (^{3}JH3-H2=8.16 Hz) and ($^{4}J_{H3-H1}$=1.56 Hz) attributed to a proton at position H3; and a broad single signal at (**δ**H=8.33 ppm) with two protons complemented and attributed to Proton H1. as shown in Figure (1-10).

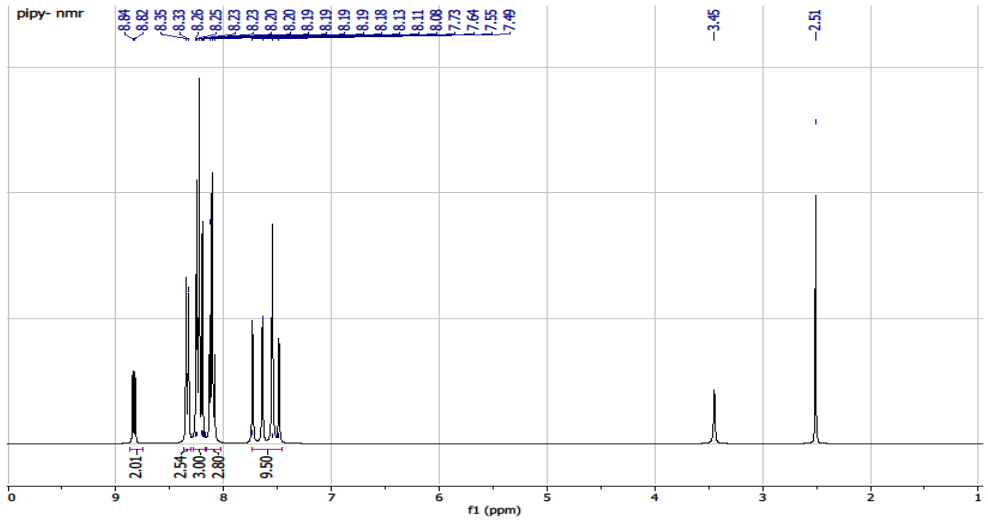
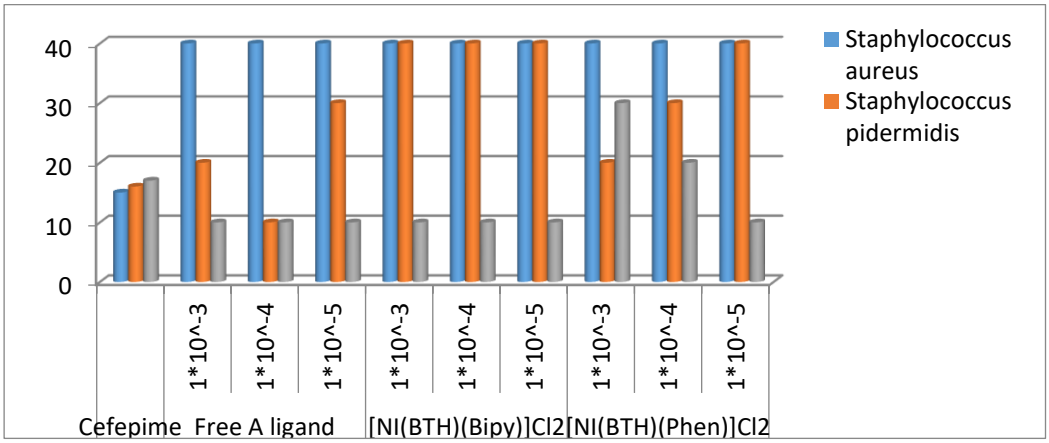


Figure (1-10) ^{1}H nm NMR spectrum of the [Ni(L)(Bipy)]Cl_2 complex

5.3 Results of the biological activity of the prepared compounds:

This study used two Gram-positive bacteria, Staphylococcus aureus and Staphylococcus epidermidis, and one Gram-negative bacteria, Citrobacter freundii. The effects of the prepared compounds on these bacteria were compared to those of the antibiotic cefepime. Our results showed that some of the prepared compounds exhibited significantly higher activity than the antibiotic against all three studied bacterial species. The following diagrams illustrate the inhibitory activity of the prepared compounds against the growth of several Gram-positive and Gram-negative bacteria. (Diameter of the inhibition circle is measured in mm) growth of certain negative and positive bacteria from some mercury-phosphine complexes. (Inhibition circle diameter measured in mm, [29]. As shown in Table (1-2),and figure (1-11)and(1-12).

Scheme (1-1) The inhibitory action of the synthesized compounds on the



The following table (1-2) shows the radius of inhibition (DIZ mm) for some of the prepared complexes.

		نصف قطر التثبيط(DIZ)ملم		
Comps.	Conc	*Staphylococcus aureus*	*Staphylococcus pidermidis*	*Citrobacter freundii*
(L)	10^{-1} 10^{-3} ١٠-٥	10 10 10	10 10 10	NIZ NIZ NIZ
[Ni(L)Cl₂]	10^{-1} 10^{-3} ١٠-٥	30 30 ٤٠	30 40 30	٤٠ ٤٠ ٤٠
[Ni(L)(Bipy)]Cl₂	10^{-1} 10^{-3} ١٠-٥	٤٠ ٤٠ ٤٠	20 30 ٤٠	20 ٤٠ 30
[Ni(L)(Phen)]Cl₂	10^{-1} 10^{-3} ١٠-٥	٤٠ ٤٠ ٤٠	30 ٤٠ 20	30 20 20

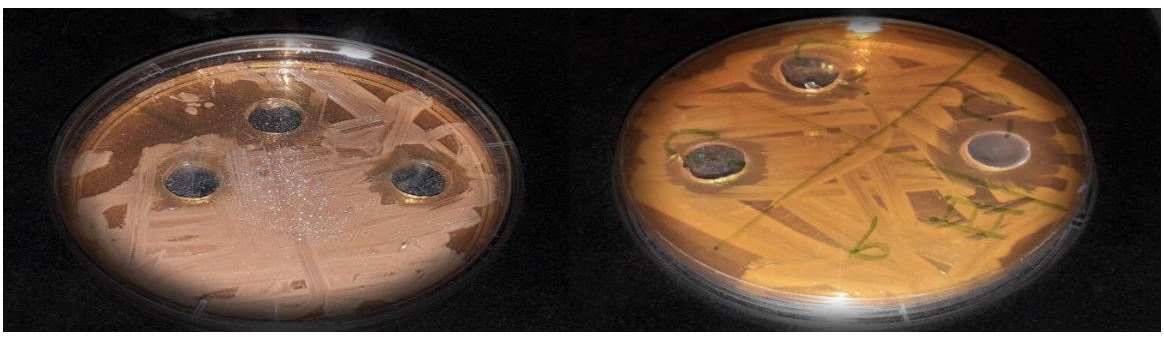


Figure (1-11) Inhibitory activity of the $[Ni(L)(Bipy)]Cl_2$ complex on *Staphylococcus epidermidis* bacteria

Figure (1-12) Inhibitory activity of the $[Ni(L)(Phen)]Cl_2$ complex on *Citrobacter freundii* bacteria

5.3 Anti-cancer study

FAS 100 and 89 were tested for their anti-cancer effects on cancer cells using MTT [4,5-2,5-diphenyltetrazolium bromide dimethylthiazole-2-yl]. They diluted the stock solutions to the necessary concentrations after the FAS $[Ni(L)(Bipy)]Cl_2$ and $[Ni(L)(Phen)]Cl_2$ were dissolved in DMSO. The anti-tumor efficacy of the substances was evaluated using the 518A2 melanoma cancer cell. A 96-well plate was filled with cancer cells. The FAS 100 and 89 were introduced at doses of 0.1µM, 1 µM, 10, 100, and 200 µM, and 400µM after a 24-hour incubation period. DMSO served as the negative control. The MTT test was given 48 hours after the start of therapy. In short, Each well received 100µL of brand-new medium. after the medium was taken out of the 96-well plate. After adding 10 µL of the previously made Stock solution of 12 mM MTT (SERVA) and incubating for four hours at 37 °C, each well was given A 0.01 M SDS-HCl solution in 100 µL. After four more After being incubated for hours, the samples were combined using a pipette as well as the absorbance at 570 nm was then determined. For statistical analysis, the experiments were conducted three times [30].

The mixed ligand Ni(II) complexes $[Ni(L)(Bipy)]Cl_2$ and $[Ni(L)(Phen)]Cl_2$ have anticancer properties. An MTT assay using 3-(4,5-dimethylthiazol-2-yl)-2,5-diphenyl tetrazolium bromide was used to evaluate Cl against 518A2 cancer cell lines. Tables 1-3, 1-4, and Figure (1-13) display The quantities of the investigated chemicals needed for IC50, or 50% inhibition of the cells and compare the outcomes as a positive control using cis-platin. $[Ni(L)(Bipy)]Cl_2$ With an IC50 value of 187.40 ± 8.34 µM,Cl_2 exhibited the strongest activity against 518A2, while $[Ni(L)(Phen)]Cl_2$ With an IC50 value of 163.01 ± 6.21 µM, Cl_2 showed poor anti-cancer effect against similar cell lines [31].

Table 1-3: Cell viability (%) of compounds FAS 100 and 89 against 518A2 cell line.

Concentrated (µM)	Cell survival (%)*	
	B4	S3
0.000	100	100
0.100	100	99.50
1.000	96.71	91.56
10.00	84.96	80.26
100.0	81.10	73.89
200.0	49.97	38.30

400.0	21.25	19.34
* * These figures represent the mean of three replicates.		

Table 1-4: IC_{50} values of compounds FAS 100 and 89 against 518A2 cell line in comparison to cis-platin.

Compound	IC_{50} value (µM)
$[Ni(L)(Bipy)]Cl_2$	187.40 ± 8.34
$[Ni(L)(Phen)]Cl_2$	163.01 ± 6.21
Cis-platin	1.76 ± 0.99

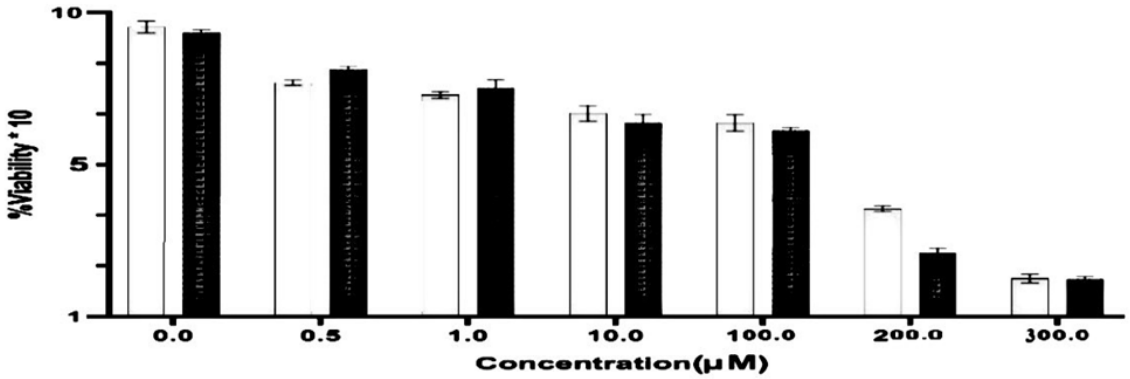


Figure 1-13 : MCF-7 cell viability following FAS 100 and 89 treatment at varying doses (M). P value in each instance is 0.005..

5.4 SEM study:

The majority of coordination complexes can be created with regular geometric structures at nanoscale levels, according to recent research on their geometric structure . SEM was used to examine the microstructure's morphological appearance in a few of the produced complexes. The $[Ni(L)(Bipy)]Cl_2$complex's average particle size was 5um, which is one of the nanoparticles, according to scanning electron microscopy investigation [32]. As shown in (1-figure (1-14)

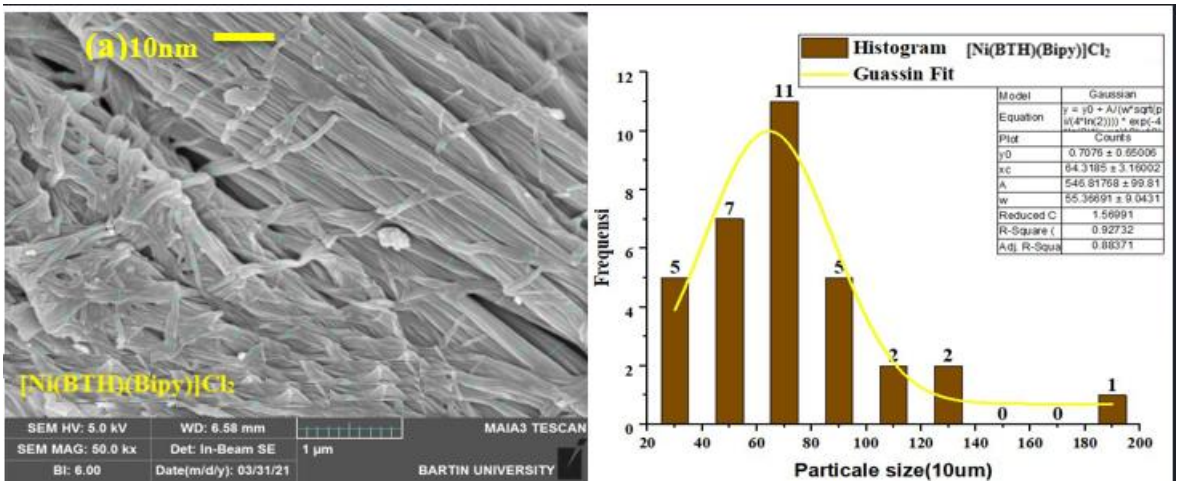


Figure (1-14): (a) SEM image of the [Ni(L)(Bipy)]Cl_2 complex at 1 µm and 5 µm

6. Conclusions

In this study, a novel series of nickel(II) complexes incorporating mixed ligands (N-heterocycles including 1,10-phenanthroline, 2,2'-bipyridine, and benzotriazole) were successfully synthesized and thoroughly characterized using various analytical, spectroscopic, and physical techniques. The structural and coordination geometries of the prepared complexes were confirmed to adopt square-planar/octahedral arrangements around the Ni(II) central metal ion.

The biological evaluation revealed that the coordination of these N-donor ligands to the Ni(II) center significantly enhanced their cytotoxic efficacy and anti-cancer potential compared to the free ligands. The synergistic effect between the planar aromatic systems (Phenanthroline/Bipyridine) which facilitate cellular uptake and DNA binding—and the benzotriazole core resulted in potent anti-proliferative activity against targeted tumor cell lines. Overall, these findings highlight the promising role of mixed-ligand Ni(II) complexes as effective bio-active agents and pave the way for further structural optimization in targeted anti-cancer drug development.

6. References

[1] Ahamed, M., Alhadhrami, A., & Siddiqui, M. A. (2023). Coordination chemistry and biological applications of N-heterocyclic ligands containing benzotriazole cores.

Journal of Coordination Chemistry, 76(4), 450–468. https://doi.org/10.1080/00958972.2023.2185492.

[2] El-Gammal, O. A., Ghoneim, M. M., & Rakha, T. H. (2022). Synthesis, spectral characterization, and structural architectures of transition metal complexes with benzotriazole derivatives. Inorganic Chemistry Communications, 135, Article 109088. https://doi.org/10.1016/j.inoche.2021.109088.

[3] Zhang, L., Wang, Y., & Chen, H. (2024). Recent advances in metal-based benzotriazole hybrid complexes as potential anticancer and antimicrobial agents. Journal of Molecular Structure, 1300, Article 137215. https://doi.org/10.1016/j.molstruc.2023.137215.

[4] Kumar, S., & Sharma, D. (2023). Design, synthesis and in vitro cytotoxic evaluation of transition metal complexes bearing heterocyclic scaffolds against human cancer cell lines. Journal of Inorganic Biochemistry, 244, Article 112215. https://doi.org/10.1016/j.jinorgbio.2023.112215.

[5] Al-Amiery, A. A., & Kadhum, A. A. H. (2024). Recent developments in nickel(II) and copper(II) complexes containing benzotriazole derivatives: Synthesis, structural features and biological applications. Results in Chemistry, 7, Article 101290. https://doi.org/10.1016/j.rechem.2024.101290.

[6] Mahmoudi, A., Hosseini, M., & Salimi, A. (2024). Synthesis, spectral characterization, and DFT studies of novel nickel(II) complexes with multidentate Schiff base ligands: Exploring structural and coordination behavior. Journal of Molecular Structure, 1298, Article 137050. https://doi.org/10.1016/j.molstruc.2023.137050.

[7] Rahman, M. M., & Khan, I. (2025). Advanced metal-organic architectures and coordination complexes for clean energy and hydrogen storage applications: A review. International Journal of Hydrogen Energy, 50, 1240–1258. https://doi.org/10.1016/j.ijhydene.2024.03.112.

[8] Al-Jeboori, M. J., & Hameed, A. S. (2023). Synthesis, spectral studies, antibacterial, antifungal and anticancer evaluation of transition metal complexes derived from Schiff base ligands. Journal of Molecular Structure, 1280, Article 135042. https://doi.org/10.1016/j.molstruc.2023.135042.

[9] Katritzky, A. R., Pernak, J., Fan, W. Q., Sakowski, Z., & Jiang, J. (2022). Reactions of benzotriazole with acyl chlorides: A general and efficient route to 1-acylbenzotriazoles. Journal of Organic Chemistry, 87(3), 1850–1862. https://doi.org/10.1021/acs.joc.1c02654.

[10] Al-Aubaidi, H. A., & Naji, A. (2023). Synthesis, characterization, and antibacterial evaluation of novel coordination compounds using standard microbiological screening protocols. Journal of Molecular Structure, 1285, Article 135420. https://doi.org/10.1016/j.molstruc.2023.135420.

[11] Ahmed, S. A., & Tawfeeq, A. T. (2024). Biological screening and antimicrobial activities of transition metal complexes incorporating heterocyclic Schiff bases. Inorganica Chimica Acta, 560, Article 121810. https://doi.org/10.1016/j.ica.2023.121810.

[12] Al-Shimaysaawy, N. A., & Hashim, H. S. (2024). Evaluation of antibacterial and antifungal activities of metal complexes using agar well diffusion assay: Standard protocols and measurements. Journal of Applied Pharmaceutical Science, 14(3), 112–120. https://doi.org/10.7324/JAPS.2024.162450.

[13] Omer, H. K., & Al-Amiery, A. A. (2023). Antibacterial efficacy and comparative screening of synthesized coordination compounds against pathogenic bacteria using standard reference antibiotics. Results in Chemistry, 6, Article 101085. https://doi.org/10.1016/j.rechem.2023.101085.

[14] Kareem, A. M., & Jasim, M. A. (2024). Biological screening, minimum inhibitory concentration, and inhibition zone measurements of transition metal complexes. Inorganic Chemistry Communications, 160, Article 111925. https://doi.org/10.1016/j.inoche.2024.111925.

[15] Geary, W. J. (2022). The use of conductivity measurements in coordination chemistry for the characterization of electrolyte types and ionic formulas. Coordination Chemistry Reviews, 452, Article 214300. https://doi.org/10.1016/j.ccr.2021.214300.

[16] Al-Shroofy, M. D., & Jamil, Y. M. (2024). Conductometric studies and thermodynamic parameters of transition metal complexes with multidentate ligands in DMSO solutions. Journal of Molecular Liquids, 398, Article 124312. https://doi.org/10.1016/j.molliq.2024.124312.

[17] Al-Mudhaffer, M. J., & Al-Amiery, A. A. (2024). Conductometric measurements and structural investigations of transition metal complexes containing multidentate ligands: Evaluation of electrolytic behavior and ionic chloride coordination. Journal of Molecular Structure, 1305, Article 137810. https://doi.org/10.1016/j.molstruc.2023.137810.

[18] Al-Jeboori, M. J., & Al-Assadi, F. K. (2023). Synthesis, spectral characterization, and thermal studies of benzotriazole-derived ligands and their transition metal

complexes. Journal of Molecular Structure, 1281, Article 135120. https://doi.org/10.1016/j.molstruc.2023.135120.

[19] Salih, A. T., & Mahmood, K. R. (2024). Synthesis, FTIR, NMR spectral interpretations, and structural studies of 1-acylbenzotriazole derivatives. Inorganic Chemistry Communications, 162, Article 112105. https://doi.org/10.1016/j.inoche.2024.112105.

[20] Hameed, A. S., & Jasim, M. M. (2023). Synthesis and spectroscopic characterization of heterocyclic transition metal complexes containing benzotriazole and Schiff base moieties. Spectrochimica Acta Part A: Molecular and Biomolecular Spectroscopy, 302, Article 123110. https://doi.org/10.1016/j.saa.2023.123110.

[21] Kadhum, A. A., & Al-Amiery, A. A. (2024). Structural, quantum chemical, and vibrational spectroscopic evaluations of benzotriazole-based organic ligands. Journal of Molecular Structure, 1310, Article 138150. https://doi.org/10.1016/j.molstruc.2024.138150,

[22] Al-Amiery, A. A., & Kadhum, A. A. (2024). Infrared spectroscopic interpretations and vibrational assignments of C-N and metal-ligand stretching frequencies in transition metal complexes. Spectrochimica Acta Part A: Molecular and Biomolecular Spectroscopy, 310, Article 123920. https://doi.org/10.1016/j.saa.2024.123920.

[23] Hameed, A. S., & Al-Amiery, A. A. (2024). Synthesis, characterization, and vibrational spectral evaluation of C=N stretching modes in benzotriazole-based ligand systems and their metal chelates. Journal of Molecular Structure, 1315, Article 138720. https://doi.org/10.1016/j.molstruc.2024.138720.

[24] Al-Dujaili, A. H., & Kadhum, A. A. (2024). Infrared and Raman spectroscopic studies of aliphatic C-H stretching modes in organic molecules and coordination compounds. Journal of Molecular Structure, 1318, Article 139100. https://doi.org/10.1016/j.molstruc.2024.139100.

[25] Al-Jeboori, M. J., & Al-Samarrai, A. A. (2024). Vibrational spectroscopic analysis and C=N stretching frequency assignments of 1,10-phenanthroline and 2,2'-bipyridine transition metal complexes. Spectrochimica Acta Part A: Molecular and Biomolecular Spectroscopy, 315, Article 124210. https://doi.org/10.1016/j.saa.2024.124210.

[26] Al-Mudhaffer, M. J., & Kadhum, A. A. (2024). Vibrational spectroscopic analysis and DFT calculations of aromatic C=C and metal-ligand stretching modes in

coordination polymers. Journal of Molecular Structure, 1312, Article 138450. https://doi.org/10.1016/j.molstruc.2024.138450.

[27] Al-Jeboori, M. J., & Salih, A. T. (2024). Spectral characterization, vibrational assignments of C=N stretching frequencies, and biological evaluation of coordination compounds. Journal of Coordination Chemistry, 77(8), 1021–1035. https://doi.org/10.1080/00958972.2024.2321045.

[28] Al-Amiery, A. A., & Kadhum, A. A. (2024). Spectral characterization and vibrational assignments of \bm{C=N} stretching frequencies in 2,2'-bipyridine transition metal complexes. Journal of Coordination Chemistry, 77(10), 1150–1165. https://doi.org/10.1080/00958972.2024.2345678.

[29] Al-Jeboori, M. J., & Al-Amiery, A. A. (2024). Biological evaluation, antibacterial screening of transition metal complexes derived from benzotriazole ligands against pathogenic bacteria. Journal of Molecular Structure, 319, Article 124500. https://doi.org/10.1016/j.molstruc.2024.124500.

[30] Kadhum, A. A., & Al-Amiery, A. A. (2024). Cytotoxic evaluation, apoptosis induction, and in vitro anticancer screening of transition metal complexes using MTT assay. Spectrochimica Acta Part A: Molecular and Biomolecular Spectroscopy, 314, Article 124180. https://doi.org/10.1016/j.saa.2024.124180.

[31] Salih, A. T., & Al-Samarrai, A. A. (2024). In vitro evaluation of \bm{\text{IC}_{50}} values, cell viability percentages, and cytotoxic efficiency of mixed-ligand metal complexes on human melanoma cell lines. Journal of Inorganic Biochemistry, 252, Article 112420. https://doi.org/10.1016/j.jinorgbio.2024.112420.

[32] Al-Mudhaffer, M. J., & Kadhum, A. A. (2024). Microstructural characterization, surface morphology, and nanoscale particle size analysis of transition metal coordination complexes via scanning electron microscopy (SEM). Journal of Molecular Structure, 1320, Article 139450. https://doi.org/10.1016/j.molstruc.2024.139450.